One-loop contributions to dark matter-nucleon scattering in a scalar and a vector DM model

Rui Santos

ISEL & CFTC-UL

Workshop on Connecting Insights in Fundamental Physics: Standard Model and Beyond

6 September 2019

with Azevedo, Duch, Grzadkowski, Huang, Iglicki

and with Glaus, Mühlleitner, Müller, Patel

Motivation

- Goal - compare two of the simplest models with dark matter candidates - one with scalar dark matter and one with vector dark matter.

- Both models have a new complex scalar singlet. Its real component mixes with the neutral component from the doublet.

- The models have the same number of particles and the same number of independent parameters.

- In this case can we distinguish the models experimentally? And if so how?

Azevedo, Duch, Grzadkowski, Huang, Iglicki, Santos, "Testing scalar versus vector dark matter", PRD99, 015017 (2019)

Azevedo, Duch, Grzadkowski, Huang, Iglicki, Santos, "One-loop contribution to dark matter-nucleon scattering in the pseudoscalar dark matter model", JHEP 1901 (2019) 138

Glaus, Mühlleitner, Müller, Patel, "Electroweak Corrections to Dark Matter Direct Detection in a Vector Dark Matter Model", arxiv 1908.09249

The models

1. Vector Dark Matter (VDM)

Dark $U(1)_X$ gauge symmetry: all SM particles are $U(1)_X$ neutral but a new complex scalar field $\mathbb{S}$ is added, which is a scalar under the SM gauge group but has unit charge under $U(1)_X$.
We force the Lagrangian to be invariant under

$$X_\mu \to -X_\mu, \quad \mathbb{S} \to \mathbb{S}^*$$

which is just the charge conjugate symmetry in the dark sector. It forbids the kinetic mixing between the SM gauge boson from $U(1)_Y$ and the dark one from $U(1)_X$. The Lagrangian is

$$\mathscr{L} = \mathscr{L}_{SM} - \frac{1}{4} X_{\mu\nu} X^{\mu\nu} + (D_\mu \mathbb{S})^\dagger (D^\mu \mathbb{S}) + \mu_S^2 \left| \mathbb{S} \right|^2 - \lambda_S \left| \mathbb{S} \right|^4 - \kappa \left| \mathbb{S} \right|^2 H^\dagger H$$

$$D_\mu = \partial_\mu + i g_X X_\mu$$

with

$$m_{DM} = g_X v_S$$

$$H = \begin{pmatrix} G^\pm \\ \frac{1}{\sqrt{2}}(v_H + h + iG_0) \end{pmatrix} \qquad \mathbb{S} = \frac{1}{\sqrt{2}}(v_S + S + iA)$$

$$\begin{pmatrix} h_1 \\ h_2 \end{pmatrix} = \begin{pmatrix} \cos\alpha & \sin\alpha \\ -\sin\alpha & \cos\alpha \end{pmatrix} \begin{pmatrix} h \\ S \end{pmatrix}$$

h is the real doublet component, S is the new real scalar component and A is the Goldstone boson related with $U(1)_X$.

HAMBYE, JHEP 0901 (2009) 028. LEBEDEV, LEE, MAMBRINI, PLB707 (2012) 570. FARZAN, AKBARIEH; JCAP 1210 (2012) 026. BAEK, KO, PARK, SENAHA; JHEP 1305 (2013) 036, ...

The models

2. Scalar Dark Matter (SDM)

The SM is extended by an extra complex scalar singlet $\mathbb{S}$ which has an intrinsic global U(1) symmetry

$$\mathbb{S} \to e^{i\alpha}\mathbb{S}$$

Then we softly break this dark U(1) symmetry to the residual Z_2 symmetry $\quad \mathbb{S} \to -\mathbb{S}$

$$\mathscr{L} = \mathscr{L}_{SM} + (D_\mu \mathbb{S})^\dagger (D^\mu \mathbb{S}) + \mu_S^2 \left|\mathbb{S}\right|^2 - \lambda_S \left|\mathbb{S}\right|^4 - \kappa \left|\mathbb{S}\right|^2 H^\dagger H + (\mu^2 \mathbb{S}^2 + \mathrm{h.c.})$$

with

$$\mathcal{M}^2 = \begin{pmatrix} 2\lambda_H v^2 & \kappa v v_S & 0 \\ \kappa v v_S & 2\lambda_S v_S^2 & 0 \\ 0 & 0 & -4\mu^2 \end{pmatrix}$$

$$H = \begin{pmatrix} G^\pm \\ \frac{1}{\sqrt{2}}(v_H + h + iG_0) \end{pmatrix} \qquad \mathbb{S} = \frac{1}{\sqrt{2}}(v_S + S + iA)$$

$$\begin{pmatrix} h_1 \\ h_2 \end{pmatrix} = \begin{pmatrix} \cos\alpha & \sin\alpha \\ -\sin\alpha & \cos\alpha \end{pmatrix} \begin{pmatrix} h \\ S \end{pmatrix}$$

h is the real doublet component, S is the new real scalar component and A is the dark matter candidate. The extra soft breaking term gives mass to A (the dark matter candidate).

Silveira, Zee; PLB161, 136 (1985). McDonald; PRD50 (1994) 36373649, ...

The models

PARTICLE CONTENT

VDM: SM + <u>vector dark matter</u> + new scalar

SDM: SM + <u>scalar dark matter</u> + new scalar

INDEPENDENT PARAMETERS

$$m_{DM}; \ \sin\alpha; \ m_2; \ v_S$$

m_{DM}: Mass of the DM particle

$\sin\alpha$: Mixing angle between doublet and singlet (real)

m_2: Mass of the second scalar

v_S: Singlet VEV

Parameter	Range
SM-Higgs—m_1	125.09 GeV
Second Higgs—m_2	[1,1000] GeV
DM—$m_{\rm DM}$	[1,1000] GeV
Singlet VEV—v_s	$[1,10^7]$ GeV
Mixing angle—α	$[-\frac{\pi}{4},\frac{\pi}{4}]$

There is obviously a 125 GeV Higgs (other scalar can be lighter and heavier).

Experimental and theoretical constraints to be discussed next

Constraints

Theoretical and collider:

Points generated with ScannerS requiring

- absolute minimum
- boundedness from below
- that perturbative unitarity holds
- S,T and U

Signal strength: gives a constraint on $\cos\alpha$

Searches: BR of Higgs to invisible below 24%

Searches: for extra scalars imposed via HiggsBounds which gives a bound that is a function of the new scalar mass and $\cos\alpha$

Constraints

Cosmological:

<u>DM abundance</u>: we require

$$(\Omega h^2)_{DM} < 0.1186$$ [Calculated with MicroOmegas]

or to be in the 5σ allowed interval from the Planck collaboration measurement

$$(\Omega h^2)_{DM}^{obs} = 0.1186 \pm 0.0020$$

<u>Direct detection</u>: we apply the latest XENON1T bounds

$$\sigma_{DM,N}^{eff} = f_{DM}\, \sigma_{DM,N} \quad \text{with} \quad f_{DM} = \frac{(\Omega h^2)_{DM}}{(\Omega h^2)_{DM}^{obs}}$$ [Fraction contributing to the scattering]

<u>Indirect detection</u>: for the DM range of interest, the Fermi-LAT upper bound on the dark matter annihilation from dwarfs is the most stringent. We use the Fermi-LAT bound on bb.

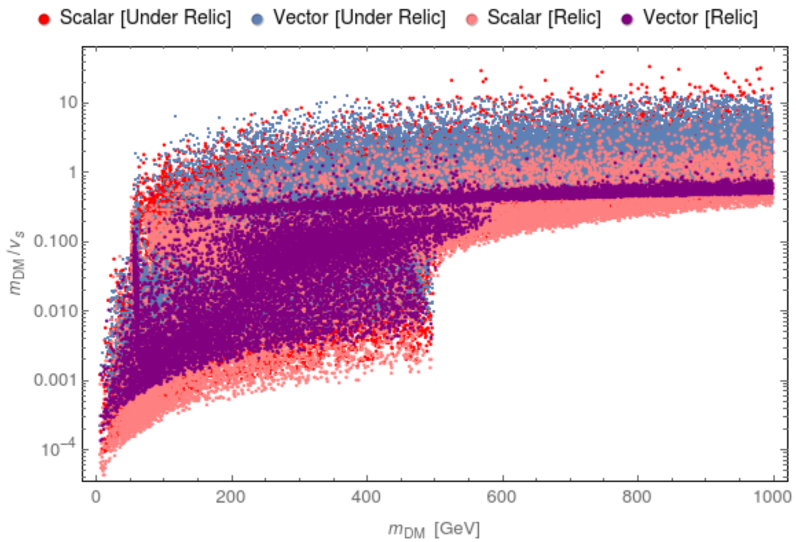

When we put together all the constraints the conclusion is that points from both models fill the entire parameter space. Plots of most measurable quantities show no difference between the models.

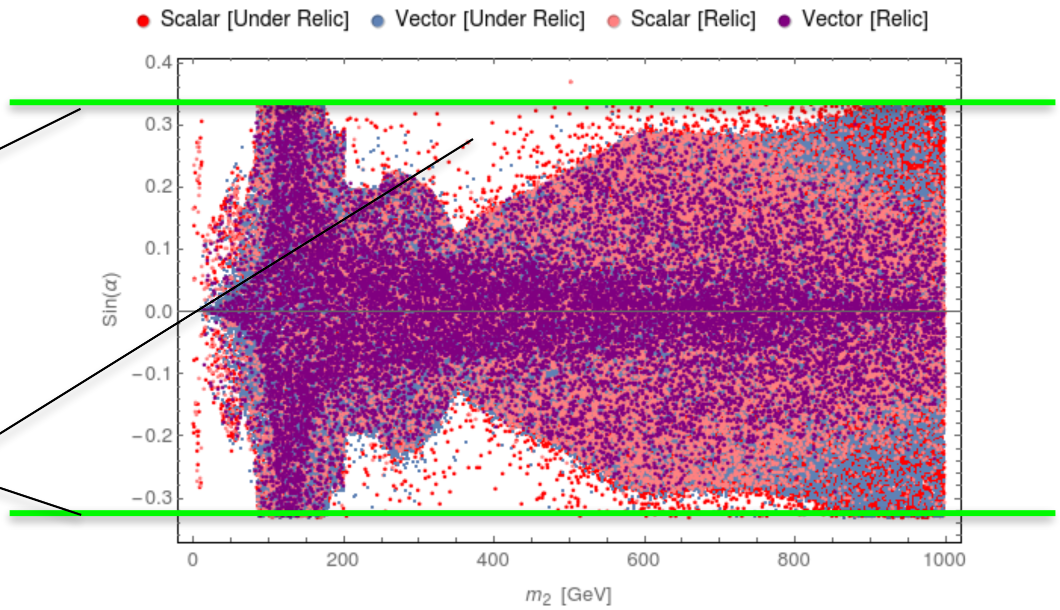

Hard bound coming from the measurement of the 125 GeV Higgs couplings

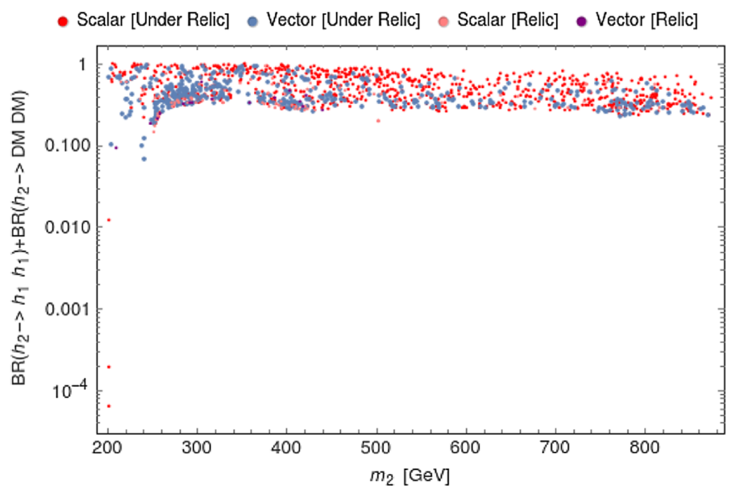

Shape comes from searches for extra scalars. Maximum close to tt threshold (Higgs production cross section via gluon fusion) has a local maximum.

The total width of the second Higgs has an extra contribution $h_2 \rightarrow$ DMDM (BR($h_2 \rightarrow ZZ$) might be suppressed) and larger allowed values of sina located outside of the pattern.

But there is a difference

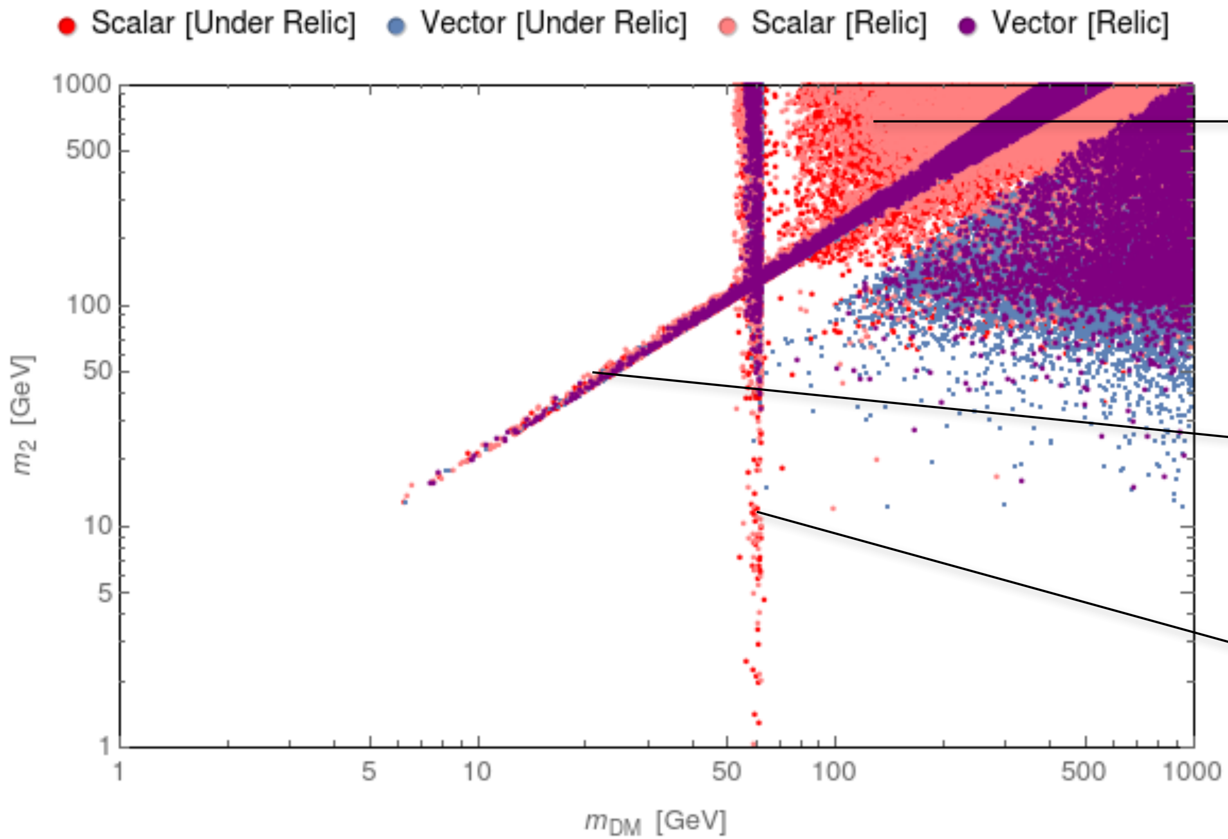

Region where only SDM survives. In this region, if we could measure the DM mass and m_2, VDM would be excluded.

Region where m_2 is close to $2m_{DM}$.

Region where m_1 is close to $2m_{DM}$.

The models coexist: kinematical enhancement by the resonance must be compensated by suppressed couplings that govern DM annihilation in the early Universe.

$m_2 \approx 2m_{DM}$ DM annihilation through the non-SM-like resonance h_2

$m_1 \approx 2m_{DM}$ DM annihilation through the non-SM-like resonance h_1

Where does this difference comes from? - Dark matter nucleon scattering at tree-level

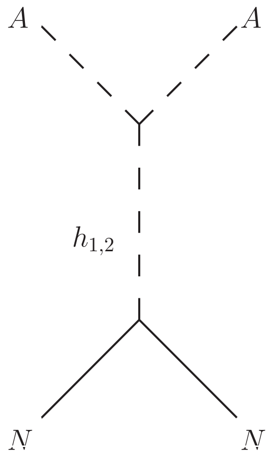

$$-i\mathcal{M}_{\text{tree}} = -\frac{i2f_N m_N}{v_H}\left(\frac{V_{AA1}c_\alpha}{q^2-m_1^2} - \frac{V_{AA2}s_\alpha}{q^2-m_2^2}\right)\bar{u}_N(p_4)u_N(p_2)$$

$$-i\mathcal{M}_{\text{tree}} \approx -i\frac{s_\alpha c_\alpha f_N m_N}{v_H v_S}\left(\frac{m_1^2-m_2^2}{m_1^2 m_2^2}\right)q^2\bar{u}_N(p_4)u_N(p_2)$$

Gross, Lebedev, Toma, PRL119 (2017) no.19, 191801

The total cross section for DM-nucleon scattering is

$$\sigma_{DM,N}^{\text{tree}} \approx \frac{\sin^2 2\alpha f_N^2}{3\pi}\frac{m_N^2\mu_{DM,N}^6}{m_{DM}^2 v_H^2 v_S^2}\frac{(m_1^2-m_2^2)^2}{m_1^4 m_2^4}v_{DM}^4 \quad \text{where} \quad \mu_{DM,N} = \frac{m_{DM}m_N}{m_{DM}+m_N}$$

Because $v_{DM} \sim 200\,\text{Km/s} \;\Rightarrow\; v_{DM}^4 \sim 10^{-13}$

It is a blind "spot" but for the entire parameter region!

$$\sigma_{DM,N}^{\text{tree}} \sim 10^{-70}\,\text{cm}^2 \ll \sigma_{DM,N}^{\text{XENON1T}} \sim 10^{-46}\,\text{cm}^2$$

So, the difference comes from Direct Detection - it is very restrictive in VDM and not restrictive at all in SDM. In fact, at tree-level

$$\sigma^{\rm tree}_{DM,N} \sim 10^{-70}\,{\rm cm}^2 \ll \sigma^{\rm XENON1T}_{DM,N} \sim 10^{-46}\,{\rm cm}^2$$

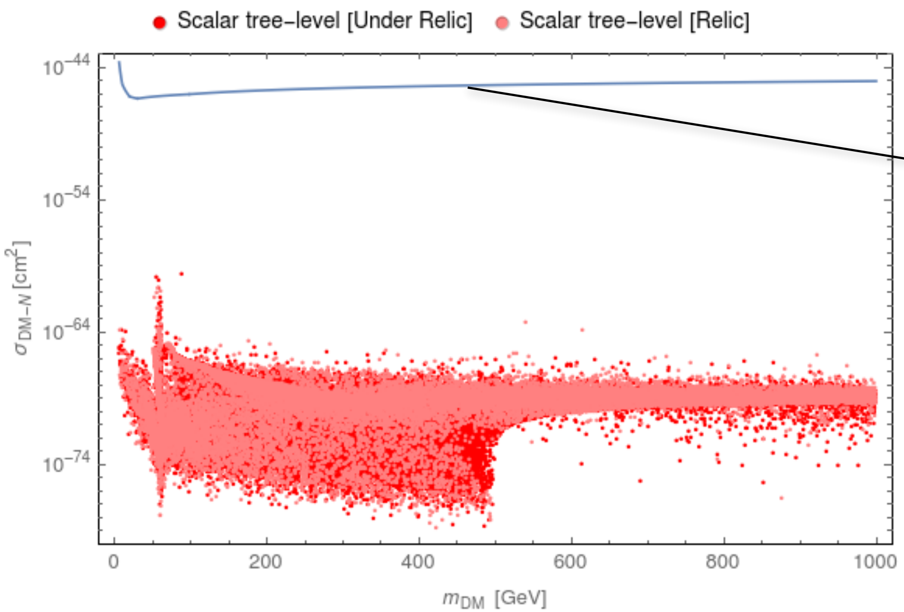

Line from the XENON1T experiment.

And what happens at one-loop?

An estimate of the cross section at one-loop was proposed

$$\sigma^{\rm tree}_{DM,N} \approx \frac{\sin^2\alpha}{64\pi^5}\frac{m_N^4 f_N^2}{m_1^4 v_H^2}\frac{m_2^4 m_{DM}^2}{v_S^6}\begin{cases}(m_2/m_{DM})^4 & m_{DM} \geq m_2\\ 1 & m_{DM} < m_2\end{cases}$$

Gross, Lebedev, Toma, PRL119 (2017) no.19, 191801

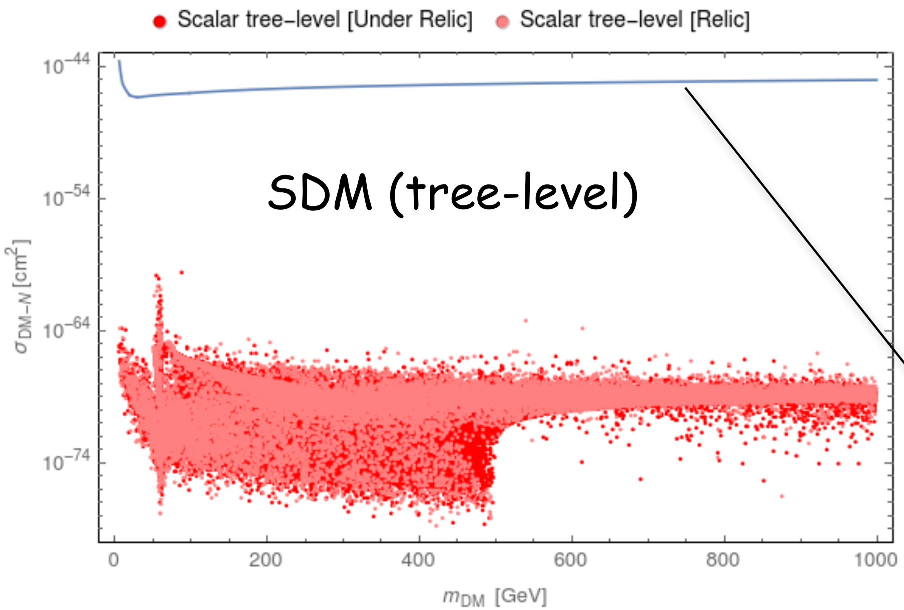

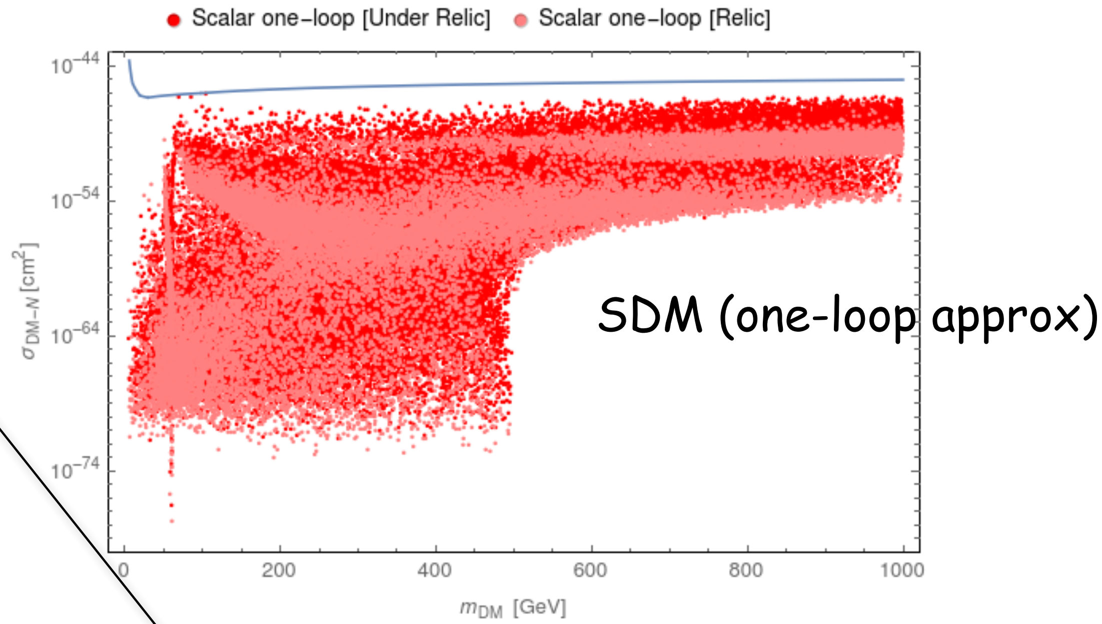

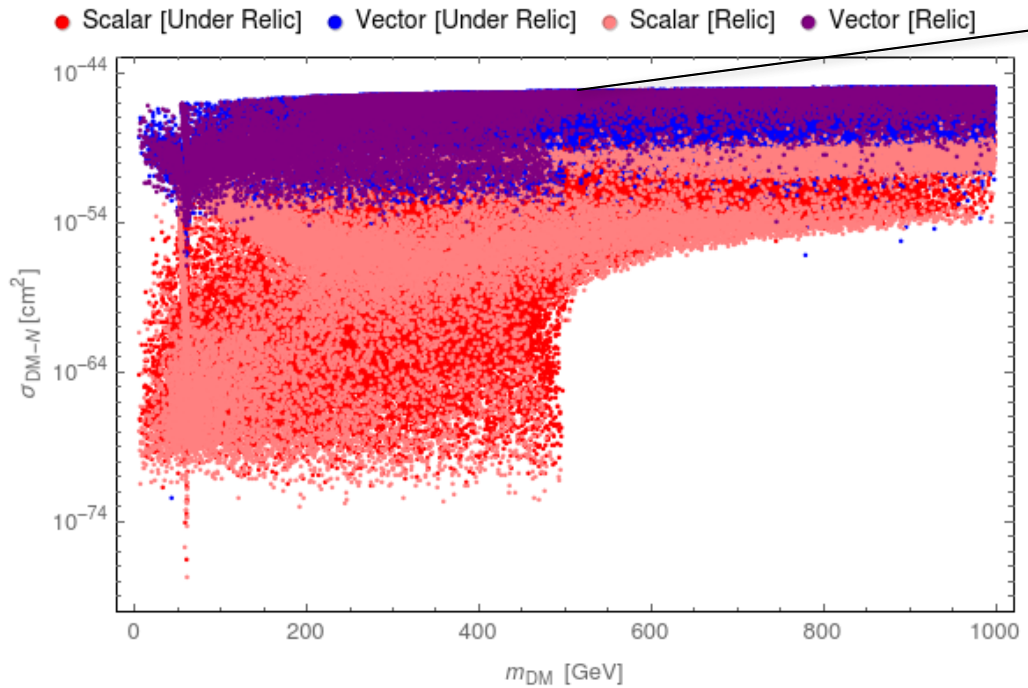

Line from the XENON1T experiment.

It is not shown, but the XENON1T line cuts a lot of the VDM points.

The one-loop calculation for SDM model

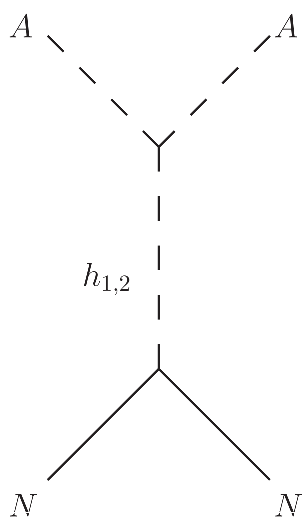

$$-i\mathcal{M}_{\text{tree}} \approx -i\frac{s_\alpha c_\alpha f_N m_N}{v_H v_S}\left(\frac{m_1^2 - m_2^2}{m_1^2 m_2^2}\right) q^2 \bar{u}_N(p_4) u_N(p_2)$$

The tree-level amplitude is proportional to q^2, this means more than 10 orders of magnitude below the XENON1T bound.

One-loop estimate brings the cross section close to the bound.

In the one-loop calculation we will still work at the nucleon level, combining the Higgs-quark and Higgs-gluon couplings to a nucleon into a single Higgs-nucleon-nucleon form factor $f_N m_N / v_H$, as we did for the tree-level diagrams.

We will work in the limit of zero momentum transfer $q^2 \to 0$ in order to simplify our calculation, which is justified by the fact that the terms proportional to q^2 are suppressed.

Corrections that survive

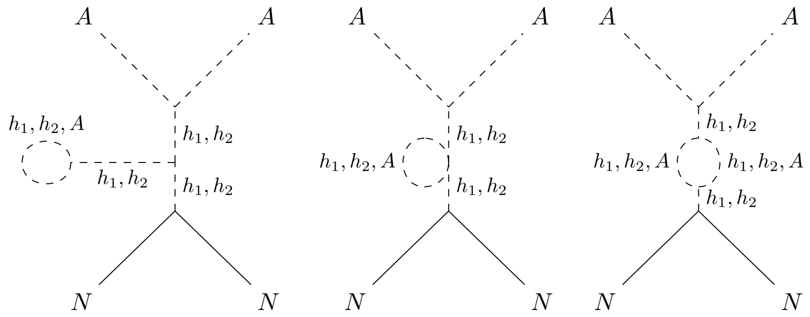

Internal scalars

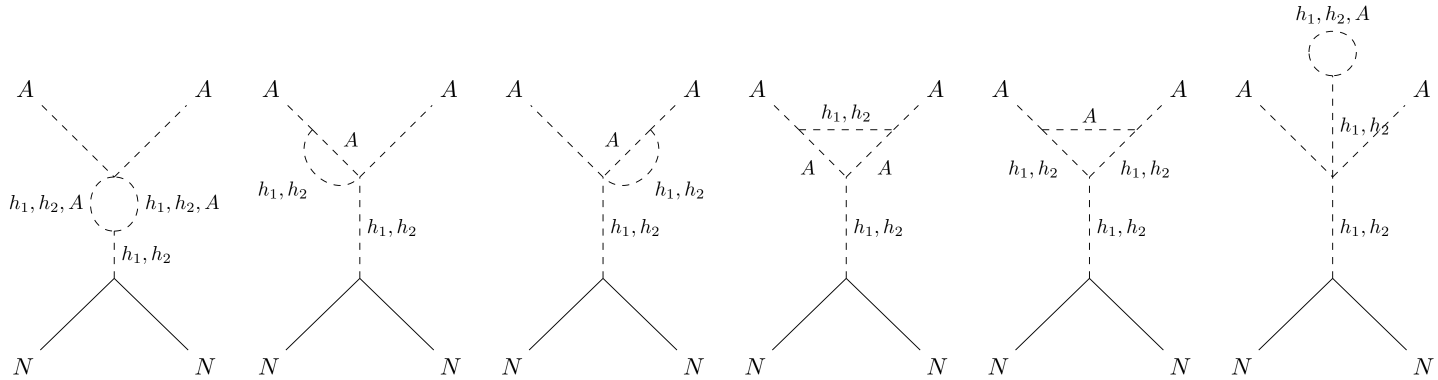

Vertex corrections

$$\mathcal{F} = -\frac{s_{2\alpha}(m_1^2 - m_2^2)m_A^2}{128\pi^2 v_H v_S^3 m_1^2 m_2^2}\big[\mathcal{A}_1 C_2(0, m_A^2, m_A^2, m_1^2, m_2^2, m_A^2) + \mathcal{A}_2 D_3(0,0,m_A^2,m_A^2,0,m_A^2,m_1^2,m_1^2,m_2^2,m_A^2) + \mathcal{A}_3 D_3(0,0,m_A^2,m_A^2,0,m_A^2,m_1^2,m_2^2,m_2^2,m_A^2)\big]$$

$$\mathcal{A}_1 \equiv 4(m_1^2 s_\alpha^2 + m_2^2 c_\alpha^2)(2m_1^2 v_H s_\alpha^2 + 2m_2^2 v_H c_\alpha^2 - m_1^2 v_S s_{2\alpha} + m_2^2 v_S s_{2\alpha}),$$
$$\mathcal{A}_2 \equiv -2m_1^4 s_\alpha[(m_1^2 + 5m_2^2)v_S c_\alpha - (m_1^2 - m_2^2)(v_S c_{3\alpha} + 4v_H s_\alpha^3)],$$
$$\mathcal{A}_3 \equiv 2m_2^4 c_\alpha[(5m_1^2 + m_2^2)v_S s_\alpha - (m_1^2 - m_2^2)(v_S s_{3\alpha} + 4v_H c_\alpha^3)].$$

$$\boxed{\sigma_{\mathrm{AN}}^{(1)} = \frac{f_N^2}{\pi v_H^2}\frac{m_N^2 \mu_{\mathrm{AN}}^2}{m_A^2}\mathcal{F}^2}$$

One-loop squared - because tree-level is zero

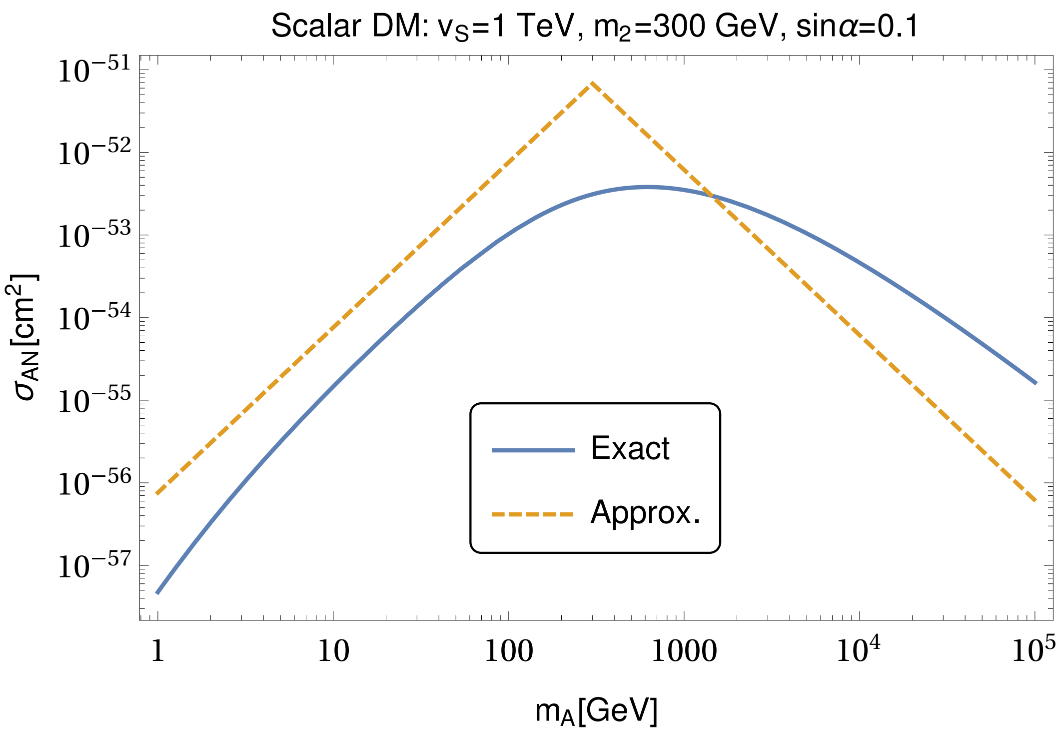

Results for the point presented as a function of the DM mass show that the approximation was good (especially in reproducing the shape.

$$\sigma^{(1)}_{\rm AN} \approx \begin{cases} \dfrac{s_\alpha^2}{64\pi^5}\dfrac{m_N^4 f_N^2}{m_1^4 v_H^2}\dfrac{m_2^8}{m_A^2 v_S^6}\,, & m_A \geq m_2 \\ \dfrac{s_\alpha^2}{64\pi^5}\dfrac{m_N^4 f_N^2}{m_1^4 v_H^2}\dfrac{m_2^4 m_A^2}{v_S^6}\,, & m_A \leq m_2 \end{cases}.$$

For this set of the parameters the curve has a maximum, $\sigma^{(1)} \sim 3 \times 10^{-53}$ cm^2 for $m_A \sim 630$ GeV.

The corresponding $\sigma^{tree} \sim 10^{-69}$–$10^{-65}$ cm^2

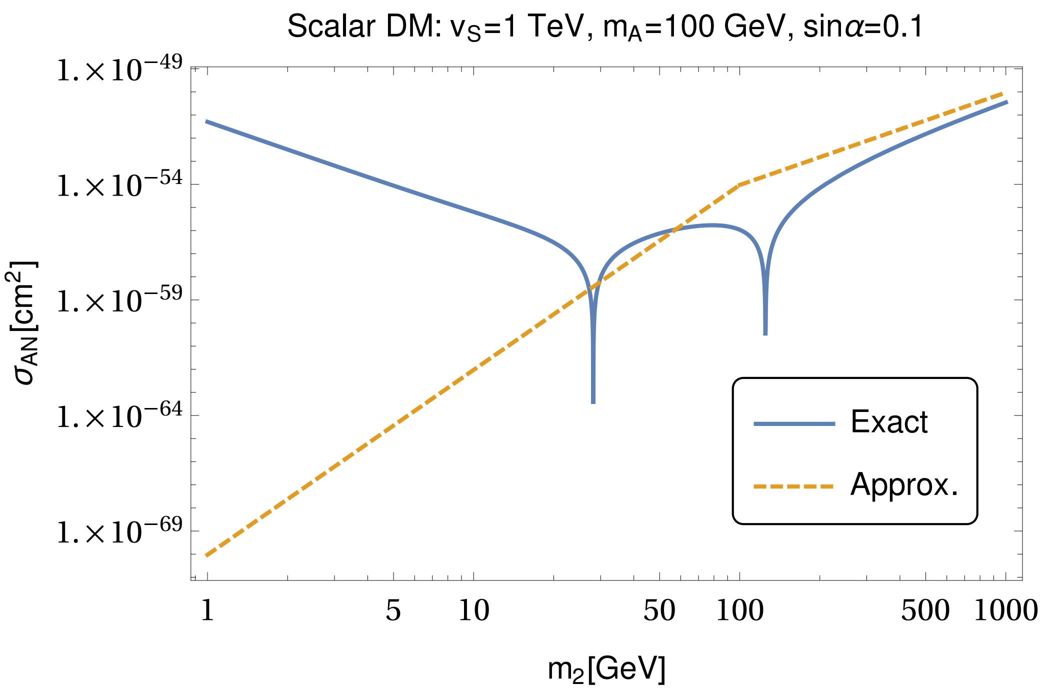

Here we can see two dips appearing in the exact calculation:

one for $m_2 = m_1$ corresponding to the vanishing of the factor $(m_1^2 - m_2^2)$ and

one at around $m_2 \sim 30$ GeV which is caused by accidental cancellation between loop integrals. The location of this dip varies with the set of parameters chosen and is a combination of all input parameters, the mass of the scalars, the angle α and v_S .

And no major changes after the exact one-loop calculation

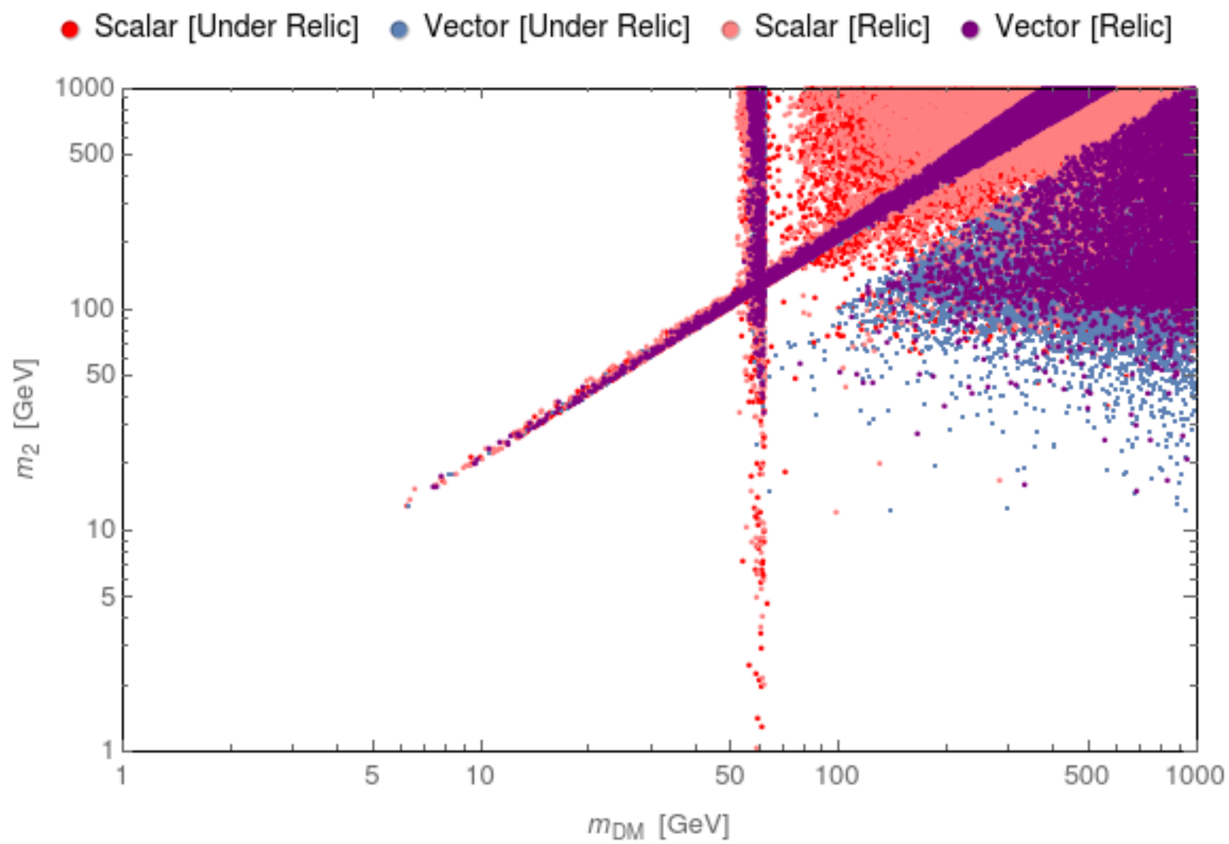

The tree-level AN recoiling amplitude vanishes in the limit of zero momentum transfer, the one-loop amplitude and F should be finite in the same limit. In other words, we do not need to renormalise the model (the set of diagrams with counterterms only is zero). Consequently, the sum of all diagrams has to be finite. .

Since the exact one-loop results lead to cross sections that are below the Xenon1T limit, the plot is exactly the same.

One-loop corrections in the VDM model

One-loop corrections in the VDM model

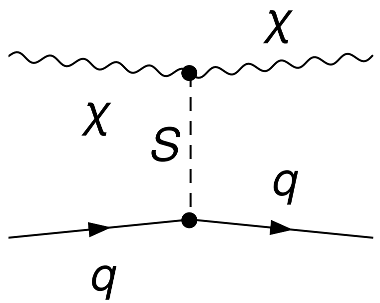

$$\mathcal{L}^{eff} = \sum_{q=u,d,s} \mathcal{L}_q^{eff} + \mathcal{L}_G^{eff}$$

We will now use an effective Lagrangian. The coefficients can be calculated at tree-level and at one-loop. The cross section (and one-loop corrections) are written in terms of these coefficients.

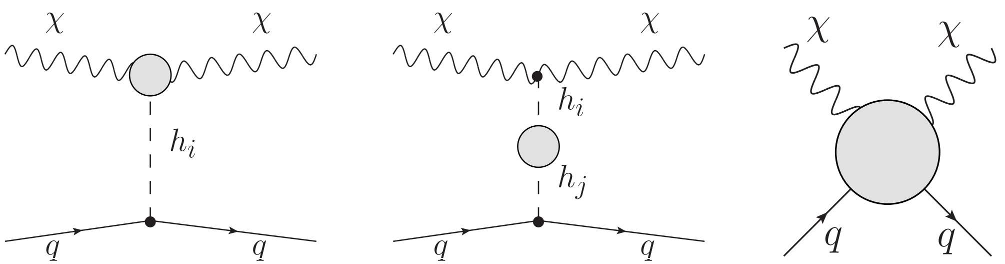

(a) Vertex Corrections (b) Mediator Corrections (c) Box Corrections

Loops are calculated - including also CT diagrams. The result can be written in terms of the form factors or of the effective Lagrangian.

Goodman, Witten, PRD31 3059 (1985); Ellis, Flores, NPB3017 883 (1988). K. Griest, PRL62 666 (1988); PRD38 2357 (1988); Srednicki, Watkins, PLB225 140 (1989); Giudice, Roulet, NPB316 429 (1989); Drees, Nojiri, PRD48 3483 (1993)

Hill, Solon, PRD91 043505 (2015)

Hisano, Ishiwata, Nagaya, Yamanaka, PTP126 435 (2011)

Abe, Fujiwara, and Hisano, JHEP 02 028 (2019)

Ertas, Kahlhoefer, JHEP06 052 (2019)

We will work in the approximation of zero momentum exchange and will consider that momentum of the incoming DM particle is equal to the momentum of the outgoing.

that is,

- Write the effective Lagrangian

$$\mathcal{L}^{\rm eff} = \sum_{q=u,d,s} \mathcal{L}^{\rm eff}_q + \mathcal{L}^{\rm eff}_G$$

$$\mathcal{L}^{\rm eff}_q = f_q \chi_\mu \chi^\mu m_q \bar{q} q + \frac{g_q}{m_\chi^2} \chi^\rho i\partial^\mu i\partial^\nu \chi_\rho \mathcal{O}^q_{\mu\nu} \,,$$
$$\mathcal{L}^{\rm eff}_G = f_G \chi_\rho \chi^\rho G^a_{\mu\nu} G^{a\,\mu\nu} \,,$$

$$\mathcal{O}^q_{\mu\nu} = \frac{1}{2} \bar{q} i \left(\partial_\mu \gamma_\nu + \partial_\nu \gamma_\mu - \frac{1}{2} \not\partial \right) q \,.$$

- Define the nucleon matrix elements

$$\begin{aligned}
\langle N | \, m_q \bar{q} q \, | N \rangle &= m_N f^N_{T_q} \\
-\frac{9\alpha_S}{8\pi} \langle N | \, G^a_{\mu\nu} G^{a,\mu\nu} \, | N \rangle &= \left(1 - \sum_{q=u,d,s} f^N_{T_q} \right) m_N = m_N f^N_{T_G} \\
\langle N(p) | \, \mathcal{O}^q_{\mu\nu} \, | N(p) \rangle &= \frac{1}{m_N} \left(p_\mu p_\nu - \frac{1}{4} m_N^2 g_{\mu\nu} \right) \left(q^N(2) + \bar{q}^N(2) \right) \,,
\end{aligned}$$

Shifman, Vainshtein, Zakharov, PLB78 443 (1978)

- And calculate the cross section

$$\sigma_N = \frac{1}{\pi} \left(\frac{m_N}{m_\chi + m_N} \right)^2 \left| f_N \right|^2 .$$

$$f_N / m_N = \sum_{q=u,d,s} f_q f^N_{T_q} + \sum_{q=u,d,s,c,b} \frac{3}{4} \left(q^N(2) + \bar{q}^N(2) \right) g_q - \frac{8\pi}{9\alpha_S} f^N_{T_G} f_G \,.$$

And now we need to get all the Wilson coefficients f_q, g_q, f_G at NLO, but before that,

Renormalisation of the VDM model

<u>INDEPENDENT PARAMETERS</u>

$$m_{DM};\ \sin\alpha;\ m_2;\ g_\chi \longrightarrow$$ (replaces Singlet VEV)

Mass of the DM particle

Mixing angle between doublet and singlet (real)

Mass of the second scalar

- Masses and fields are renormalised with on-shell conditions

$$\delta m_\chi^2 = \mathrm{Re}\,\Sigma^T_{\chi\chi}\left(m_\chi^2\right) \qquad \delta Z_{\chi\chi} = -\mathrm{Re}\frac{\partial \Sigma^2_{\chi\chi}(p^2)}{\partial p^2}\bigg|_{p^2=m_\chi^2}$$

$$\delta m_{h_i}^2 = \mathrm{Re}\big[\Sigma_{h_ih_i}(m_{h_i}^2) - \delta T_{h_ih_i}\big] \qquad \delta Z_{h_ih_i} = -\mathrm{Re}\left[\frac{\partial \Sigma_{h_ih_i}(p^2)}{\partial p^2}\right]_{p^2=m_{h_i}^2} \qquad \delta Z_{h_ih_j} = \frac{2}{m_{h_i}^2 - m_{h_j}^2}\mathrm{Re}\Big[\Sigma_{h_ih_j}(m_{h_j}^2) - \delta T_{h_ih_j}\Big]\,, \quad i \neq j$$

- The dark coupling is renormalised $\overline{MS}$

$$\delta g_\chi\big|_\varepsilon = \frac{g_\chi^3}{96\pi^2}\Delta_\varepsilon\,,$$

with $\Delta_\varepsilon = \frac{1}{\varepsilon} - \gamma_E + \ln 4\pi$, and γ_E is the Euler-Mascheroni constant.

Mixing angle is renormalised via

PILAFTSIS, NPB504, 61 (1997)

KANEMURA, OKADA, SENAHA, YUAN, PRD70 115002 (2004)

KRAUSE, LORENZ, MUHLLEITNER, RS, ZIESCHE, JHEP 1609 143 (2016)

$$\begin{pmatrix} h_1 \\ h_2 \end{pmatrix} = R(\alpha + \delta\alpha)\sqrt{Z_\Phi}\begin{pmatrix} \Phi_H \\ \Phi_S \end{pmatrix}$$

Gauge to mass eigenstates

$$R(\alpha + \delta\alpha)\sqrt{Z_\Phi}\begin{pmatrix} \Phi_H \\ \Phi_S \end{pmatrix} = \underbrace{R(\delta\alpha)R(\alpha)\sqrt{Z_\Phi}R(\alpha)^T}_{\stackrel{!}{=}\sqrt{Z_H}} R(\alpha)\begin{pmatrix} \Phi_H \\ \Phi_S \end{pmatrix} + \mathcal{O}(\delta\alpha^2) = \sqrt{Z_H}\begin{pmatrix} h_1 \\ h_2 \end{pmatrix}$$

$$\sqrt{Z_H} = R(\delta\alpha)\begin{pmatrix} 1 + \frac{\delta Z_{h_1h_1}}{2} & \delta C_h \\ \delta C_h & 1 + \frac{\delta Z_{h_2h_2}}{2} \end{pmatrix} \approx \begin{pmatrix} 1 + \frac{\delta Z_{h_1h_1}}{2} & \delta C_h + \delta\alpha \\ \delta C_h - \delta\alpha & 1 + \frac{\delta Z_{h_2h_2}}{2} \end{pmatrix}$$

Expand in the rotation angle

$$\frac{\delta Z_{h_1h_2}}{2} \stackrel{!}{=} \delta C_h + \delta\alpha \qquad \text{and} \qquad \frac{\delta Z_{h_2h_1}}{2} \stackrel{!}{=} \delta C_h - \delta\alpha$$

Using on-shell conditions

$$\boxed{\begin{aligned} \delta\alpha &= \frac{1}{4}\left(\delta Z_{h_1h_2} - \delta Z_{h_2h_1}\right) \\ &= \frac{1}{2(m_{h_1}^2 - m_{h_2}^2)}\mathrm{Re}\Big(\Sigma_{h_1h_2}(m_{h_1}^2) + \Sigma_{h_1h_2}(m_{h_2}^2) - 2\delta T_{h_1h_2}\Big)\ . \end{aligned}}$$

Tried other schemes for the angles, $\overline{MS}$ and process dependent

$$\mathcal{A}^{\mathrm{NLO,weak}}_{h\to\tau\tau} \stackrel{!}{=} \mathcal{A}^{\mathrm{LO}}_{h\to\tau\tau} \qquad \delta\alpha = \left(\frac{2m_W}{g m_\tau \cos\alpha}\right)\left[\mathcal{A}^{\mathrm{virt,weak}} + \mathcal{A}^{\mathrm{ct}}\big|_{\delta\alpha=0}\right]$$

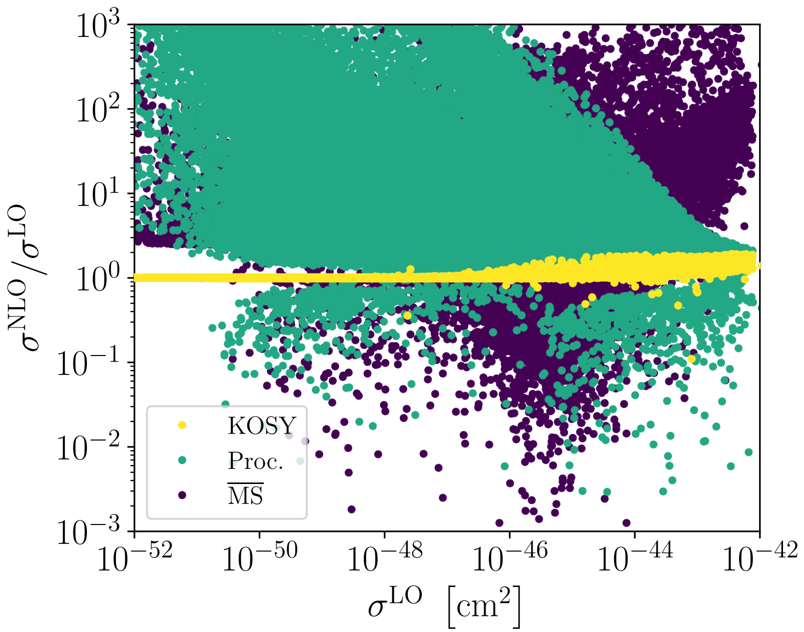

The uncertainty due to missing higher-order corrections can be estimated by varying the renormalisation scheme or by varying the renormalisation scale.

The comparison with the other two renormalisation schemes makes no sense as the latter lead to unacceptably large corrections.

The variation of the renormalisation scale (for the dark gauge coupling) between 1/2 and 2 times the scale μ_0 in the $\overline{MS}$ scheme leads to a variation of the NLO cross section of about 16% - in contrast to the unphysical large corrections that are to be traced back to the blowing-up of the MS counterterm of α.

Back to the coefficients

- Vertex corrections $\chi\chi h_i$

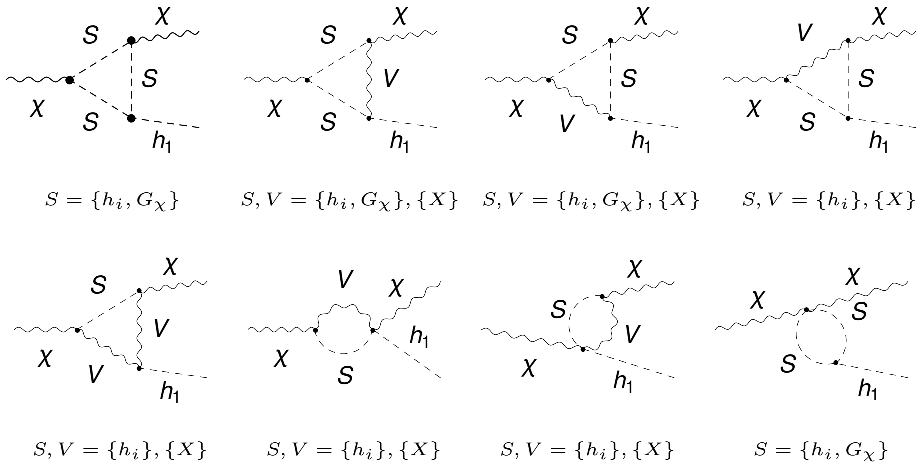

$$\boxed{i\mathcal{A}^{\rm NLO}_{\chi\chi h_i}} = i\mathcal{A}^{\rm LO}_{\chi\chi h_i} + \boxed{i\mathcal{A}^{\rm VC}_{\chi\chi h_i} + i\mathcal{A}^{\rm CT}_{\chi\chi h_i}}$$

We write the amplitude as a decay $\chi \to \chi h_i$ to extract the relevant terms.

$$i\mathcal{A}^{\rm LO}_{\chi\chi h_i} = g_{\chi\chi h_i}\varepsilon(p)\cdot\varepsilon^*(p) = 2g_\chi m_\chi \varepsilon(p)\cdot\varepsilon^*(p)\begin{cases}\sin\alpha\,, & i=1\\ \cos\alpha\,, & i=2\end{cases}$$

Loops are calculated - virtual corrections and CT diagrams are included. CT terms have the same structure as the tree-level

$$i\mathcal{A}^{\rm CT}_{\chi\to\chi h_1} = \left[\frac{1}{2}\left(g_{\chi\chi h_2}\delta Z_{h_2h_1} + g_{\chi\chi h_1}\delta Z_{h_1h_1}\right) + g_{\chi\chi h_1}\delta Z_{\chi\chi} + \delta g_{\chi\chi h_1}\right]\varepsilon(p)\cdot\varepsilon^*(p)$$

$$i\mathcal{A}^{\rm CT}_{\chi\to\chi h_2} = \left[\frac{1}{2}\left(g_{\chi\chi h_1}\delta Z_{h_1h_2} + g_{\chi\chi h_2}\delta Z_{h_2h_2}\right) + g_{\chi\chi h_2}\delta Z_{\chi\chi} + \delta g_{\chi\chi h_2}\right]\varepsilon(p)\cdot\varepsilon^*(p)$$

and virtual corrections have two terms

$$i\mathcal{A}^{\rm NLO} = (\dots)\underbrace{\varepsilon(p_{\rm in})\cdot\varepsilon^*(p_{\rm out})}_{\sim{\rm LO}} + (\dots)\underbrace{(p_{\rm in}\cdot\varepsilon^*(p_{\rm out}))\,(p_{\rm out}\cdot\varepsilon(p_{\rm in}))}_{\sim{\rm NLO}}$$

And since we work in the approximation that the momentum of the incoming DM particle is equal to the momentum of the outgoing DM particle, the LO and NLO contributions have the same structure.

FeynArts, Hahn, CPC140 418 (2001)
FeynCalc, Mertig, Bohm, Denner , CPC64 345 (1991)
Sarah, Staub, CPC185 1773 (2014)
Collier, Denner, Dittmaier, Hofer, CPC212 220 (2017)

Mediator corrections

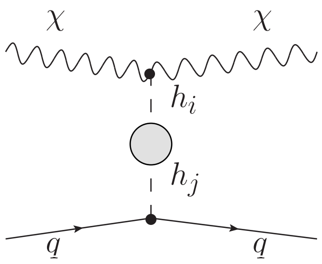

Again because we are working in the approximation of zero momentum exchange the contribution from the mediators can be written as

$$\Delta_{h_i h_j} = -\frac{\hat{\Sigma}_{h_i h_j}(p^2=0)}{m_{h_i}^2 m_{h_j}^2}$$

with

$$\begin{pmatrix} \hat{\Sigma}_{h_1 h_1} & \hat{\Sigma}_{h_1 h_2} \\ \hat{\Sigma}_{h_2 h_1} & \hat{\Sigma}_{h_2 h_2} \end{pmatrix} \equiv \hat{\Sigma}(p^2) = \Sigma(p^2) - \delta m^2 - \delta T + \frac{\delta Z}{2}\left(p^2 - \mathcal{M}^2\right) + \left(p^2 - \mathcal{M}^2\right)\frac{\delta Z}{2}$$

Projecting the one-loop correction on the corresponding tensor structure we obtain the one-loop correction to the Wilson coefficient of the operator $m_q \chi\chi\bar{q}q$ induced by the mediator corrections as

$$f_q^{\rm med} = \frac{g g_\chi m_\chi}{2 m_W} \sum_{i,j} R_{\alpha,i2} R_{\alpha,j1} \Delta_{h_i h_j}$$

and the rotation matrix defined by

$$\begin{pmatrix} h_1 \\ h_2 \end{pmatrix} = R_\alpha \begin{pmatrix} \Phi_H \\ \Phi_S \end{pmatrix} \equiv \begin{pmatrix} \cos\alpha & \sin\alpha \\ -\sin\alpha & \cos\alpha \end{pmatrix} \begin{pmatrix} \Phi_H \\ \Phi_S \end{pmatrix}$$

Box corrections

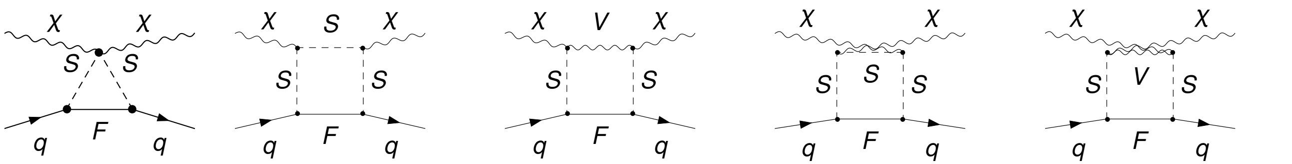

$F,S=\{q\},\{h_i\}$ $F,S=\{q\},\{h_i,G_\chi\}$ $F,S,V=\{q\},\{h_i,G_\chi\},\{X\}$ $F,S=\{q\},\{h_i\}$ $F,S,V=\{q\},\{h_i,G_\chi\},\{X\}$

Just do the calculation - nothing special here! But also need to consider

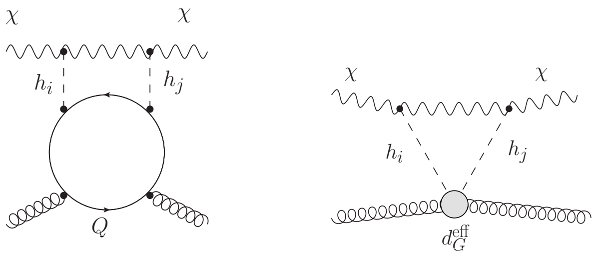

Integrating out the top quark field

$$\mathcal{L}^{hhGG}=\frac{1}{2}d_G^{\rm eff}h_ih_j\frac{\alpha_S}{12\pi}G^a_{\mu\nu}G^{a\,\mu\nu}$$

We end up with the effective Lagrangian

ABE, FUJIWARA, HISANO, JHEP 02, 028 (2019)

ERTAS, KAHLHOEFER, 1902.11070

$$\mathcal{L}_{\rm eff}\supset\left(d_G^{\rm eff}\right)_{ij}C_\triangle^{ij}\chi_\mu\chi^\mu\frac{-\alpha_S}{12\pi}G^a_{\mu\nu}G^{a\,\mu\nu}\,,$$

where $C_\triangle^{ij}$ is the contribution from the triangle (right). Finally the corresponding Wilson coefficient is

$$f_G^{\rm top}=\left(d_G^{\rm eff}\right)_{ij}C_\triangle^{ij}\frac{-\alpha_S}{12\pi}\,.$$

The NLO EW SI cross section can be obtained using the one-loop form factor

$$\frac{f_N^{\rm NLO}}{m_N} = \sum_{q=u,d,s} f_q^{\rm NLO} f_{T_q}^N + \sum_{q=u,d,s,c,b} \frac{3}{4}\left(q(2)+\bar{q}(2)\right) g_q^{\rm NLO} - \frac{8\pi}{9\alpha_S} f_{T_G}^N f_G^{\rm NLO}$$

with the Wilson coefficients at one-loop given by

$$\begin{aligned} f_q^{\rm NLO} &= f_q^{\rm vertex} + f_q^{\rm med} + f_q^{\rm box} \\ g_q^{\rm NLO} &= g_q^{box} \\ f_G^{\rm NLO} &= \boxed{-\frac{\alpha_S}{12\pi} \sum_{q=c,b,t} \left(f_q^{\rm vertex} + f_q^{\rm med}\right)} + \boxed{f_G^{\rm top}} \end{aligned}$$

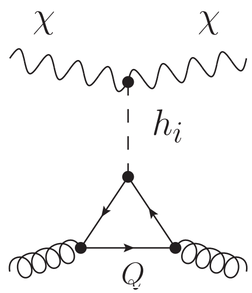

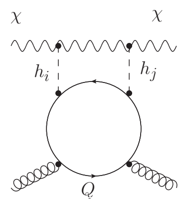

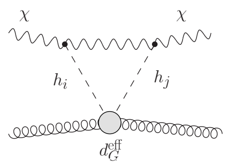

The LO form factor is given by

$$\frac{f_N^{\rm LO}}{m_N} = f_q^{\rm LO}\left[\sum_{q=u,d,s} f_{T_q}^N + \sum_{q=c,b,t} \frac{2}{27} f_{T_G}^N\right]$$

$$f_q = \frac{1}{2}\frac{g g_\chi}{m_W}\frac{\sin(2\alpha)}{2}\frac{m_{h_1}^2 - m_{h_2}^2}{m_{h_1}^2 m_{h_2}^2} m_\chi\,, \quad q = u,d,s,c,b,t$$

And the cross section at one-loop is

$$\sigma_N = \frac{1}{\pi}\left(\frac{m_N}{m_\chi + m_N}\right)^2 \left[|f_N^{\rm LO}|^2 + 2{\rm Re}\left(f_N^{\rm LO} f_N^{\rm NLO*}\right)\right]$$

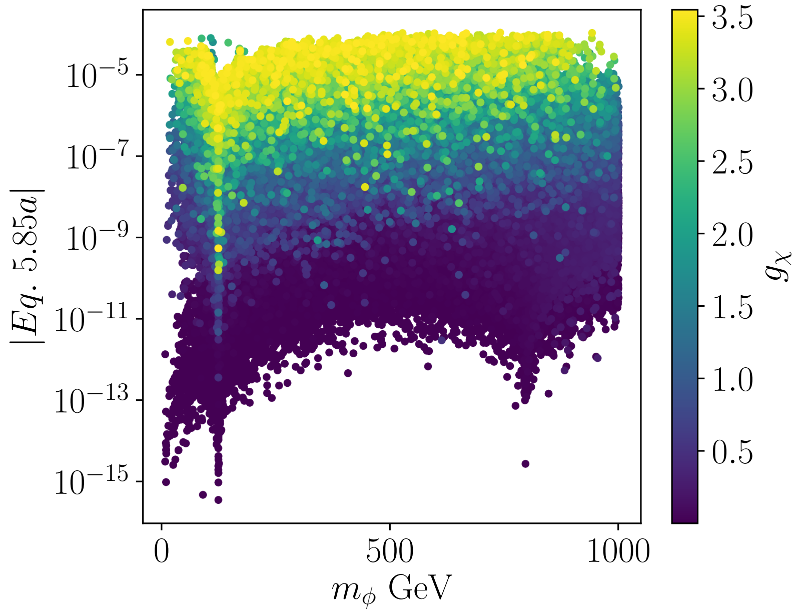

Wilson coefficient at one-loop as a function of the non-125 scalar (in units of GeV^{-2}) with the dark gauge coupling in the colour bar.

$$f_q^{\rm NLO} = f_q^{\rm vertex} + f_q^{\rm med} + f_q^{\rm box} \tag{5.85a}$$

$$g_q^{\rm NLO} = g_q^{box} \tag{5.85b}$$

$$f_G^{\rm NLO} = -\frac{\alpha_S}{12\pi} \sum_{q=c,b,t} \left(f_q^{\rm vertex} + f_q^{\rm med} \right) + f_G^{\rm top}\,. \tag{5.85c}$$

Largest contributions come from f_q^{NLO}

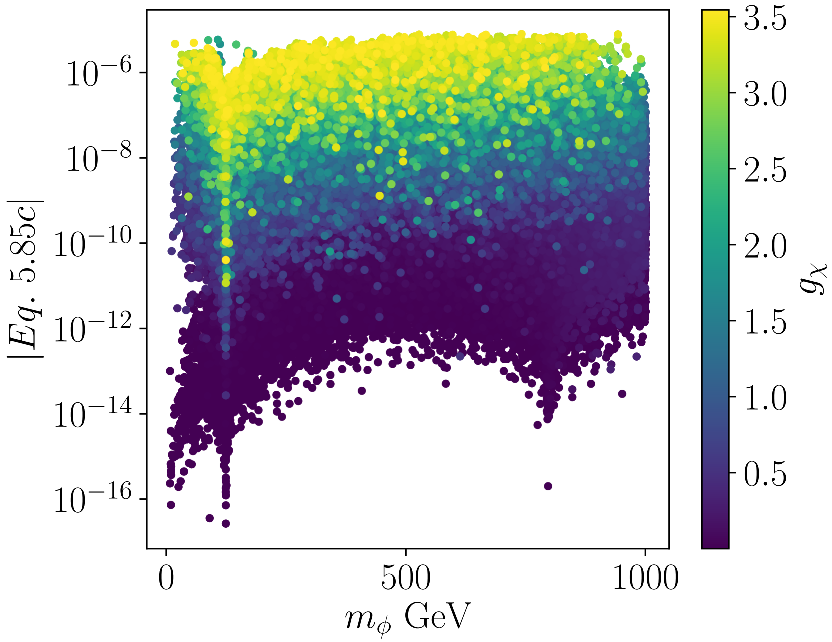

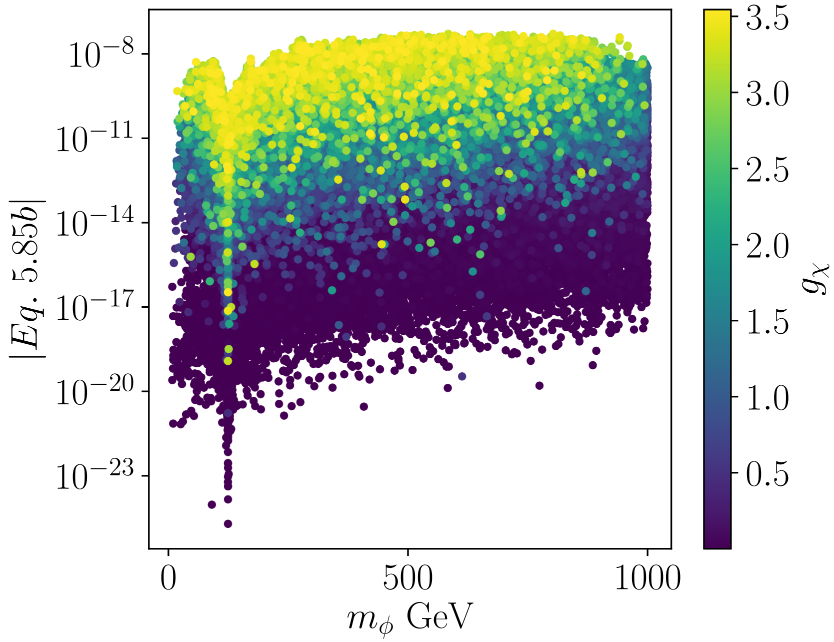

$$\frac{f_N^{\rm NLO}}{m_N} = \sum_{q=u,d,s} f_q^{\rm NLO} f_{T_q}^N + \sum_{q=u,d,s,c,b} \frac{3}{4} \left(q(2) + \bar{q}(2) \right) g_q^{\rm NLO} - \frac{8\pi}{9\alpha_S} f_{T_G}^N f_G^{\rm NLO}$$

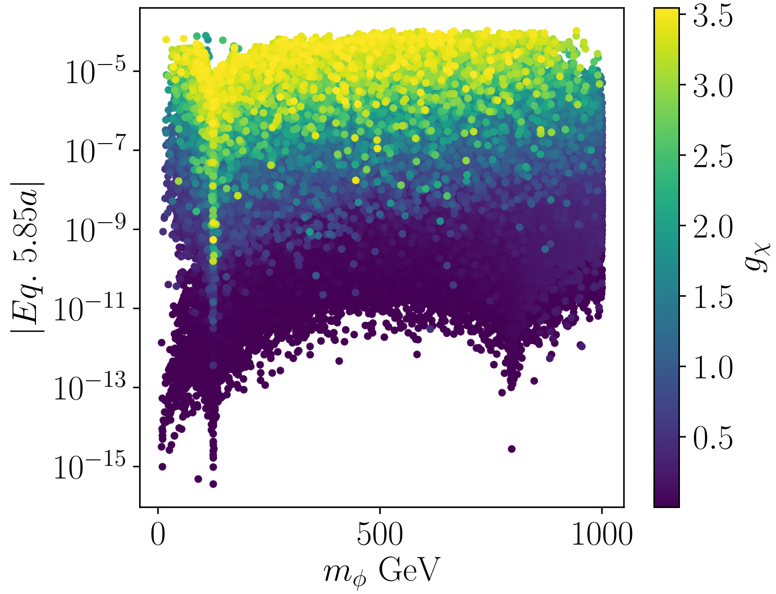

Wilson coefficient at one-loop as a function of the non-125 scalar (in units of GeV^{-2}) with the dark gauge coupling in the colour bar.

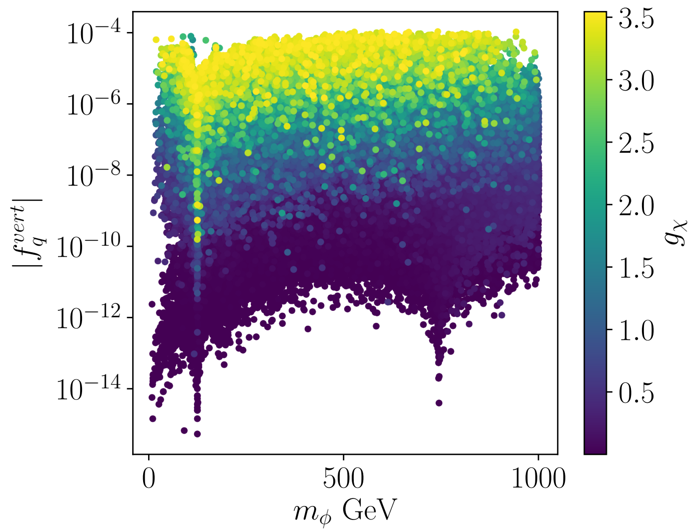

$$f_q^{\rm NLO} = f_q^{\rm vertex} + f_q^{\rm med} + f_q^{\rm box}$$

Largest contribution to f_q^{NLO} comes from f_q^{vert} but are smaller than the total.

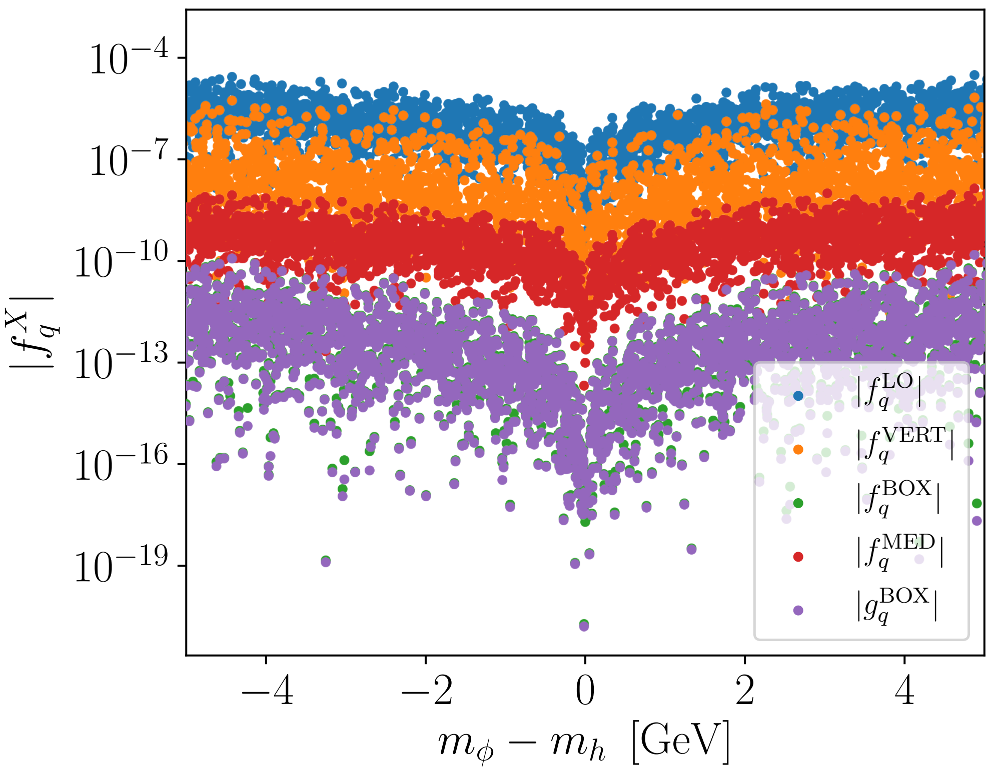

Different contributions to the cross section with LO being the largest followed by the vertex contribution.

Even for small g_χ the vertex contribution dominates except for a few points where mediator take the lead - in those cases the LO is larger by several orders of magnitude.

NLO vs. LO results for the VDM model

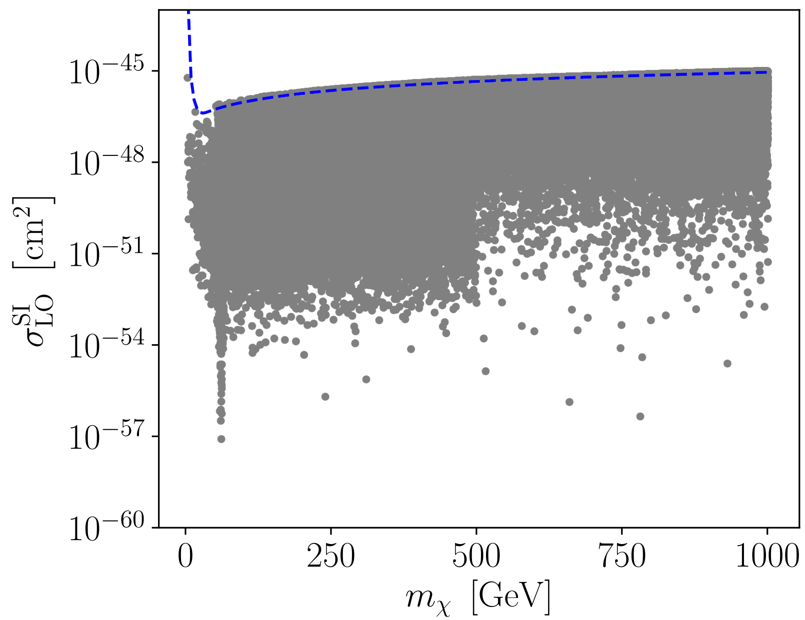

We start with points that at LO have passed all the theoretical and experimental constraints.

Both the LO and the NLO contribution to the SI direct detection cross section are proportional to f^{LO} and therefore proportional to g_χ, $\sin 2\alpha$ and $m_h^2 - m_\chi^2$.

Biggest contribution comes from the triangle diagrams which are proportional to g_χ^3 at one-loop.

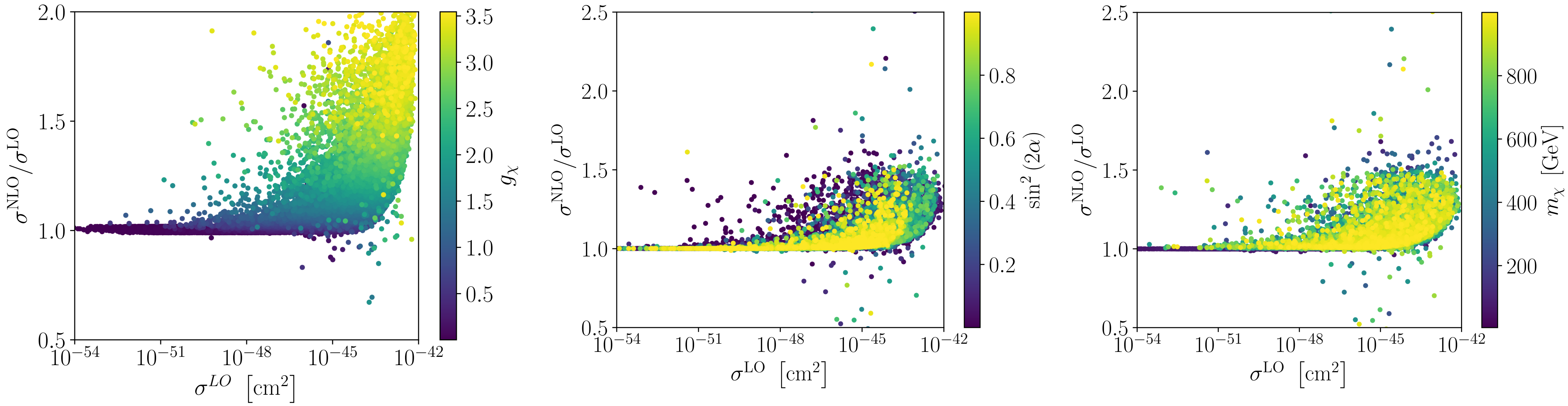

In the plots below we see the enhancement (only) with the dark coupling constant. The ratio between NLO and LO increases like g_χ.

NLO vs. LO results for the VDM model

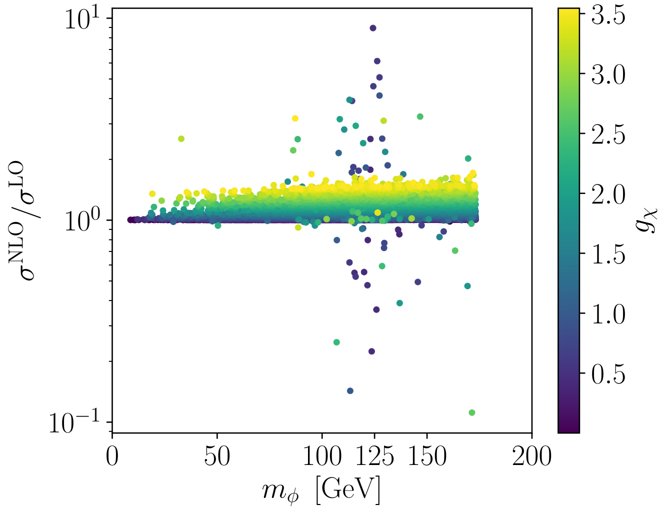

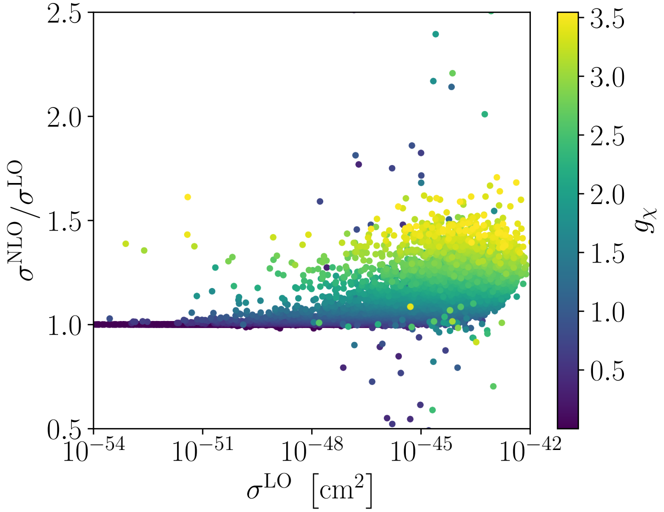

The K-factor is mostly positive and the bulk of K-factor values ranges between 1 and about 2.3.

$$f_q = \frac{1}{2}\frac{g g_\chi}{m_W}\frac{\sin(2\alpha)}{2}\frac{m_{h_1}^2 - m_{h_2}^2}{m_{h_1}^2 m_{h_2}^2} m_\chi \, ;$$

Points with $m_\varphi \approx m_h$ and K-factors where $|K| > 2.5$ are excluded. For $m_\varphi \approx m_h$ the interference effects between the h and φ contributions, largely increase the (dominant) vertex contribution. Depending on the its sign the NLO cross section is largely increased or suppressed, and the NLO results are therefore no longer reliable. Two-loop contributions might lead to a better perturbative convergence.

The blind spots at LO and at NLO are the same.

In our scan we did not find any other points where a specific parameter combination would lead to an accidental suppression at LO that is removed at NLO.

There is a further blind spot when α = 0. In this case the SM-like Higgs boson has exactly SM-like couplings and the new scalar only couples to the Higgs and to dark matter. The SM-like Higgs decouples from dark matter and we may end up with two dark matter candidates with the second scalar being metastable.

NLO vs. LO results for the VDM model

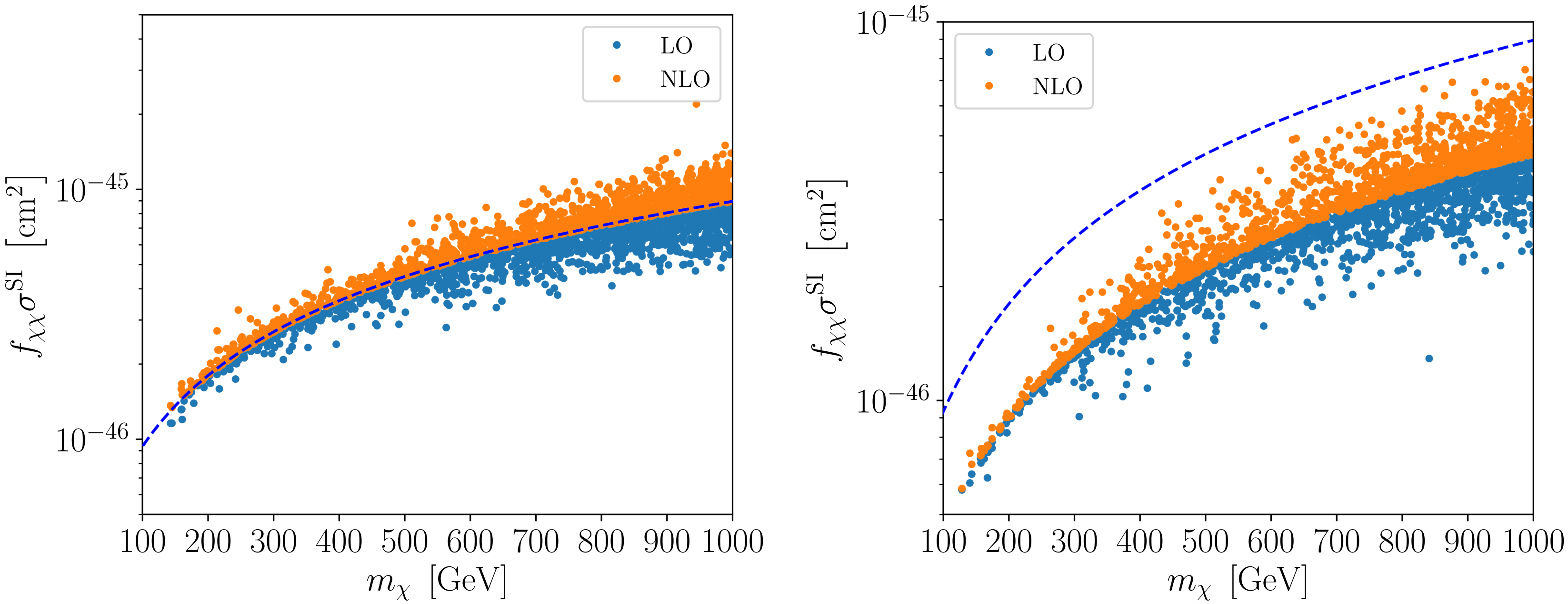

To understand the changes relative to exclusion in parameter space we have chosen two set of points.

Left: points that are not excluded at LO but are excluded at NLO.

Right: points that are far way from exclusion but are pushed closed to the bound at NLO.

The overall picture

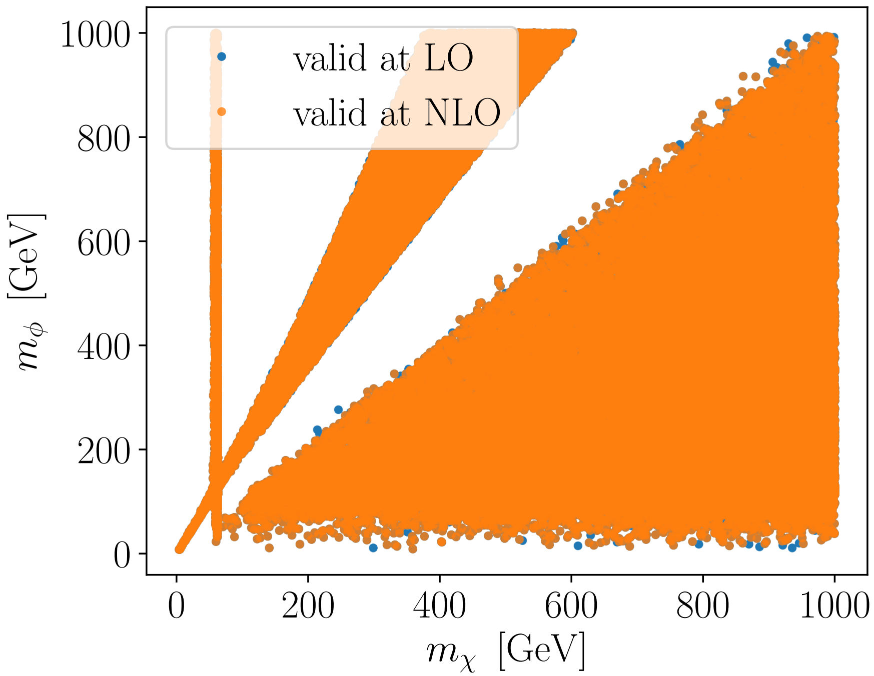

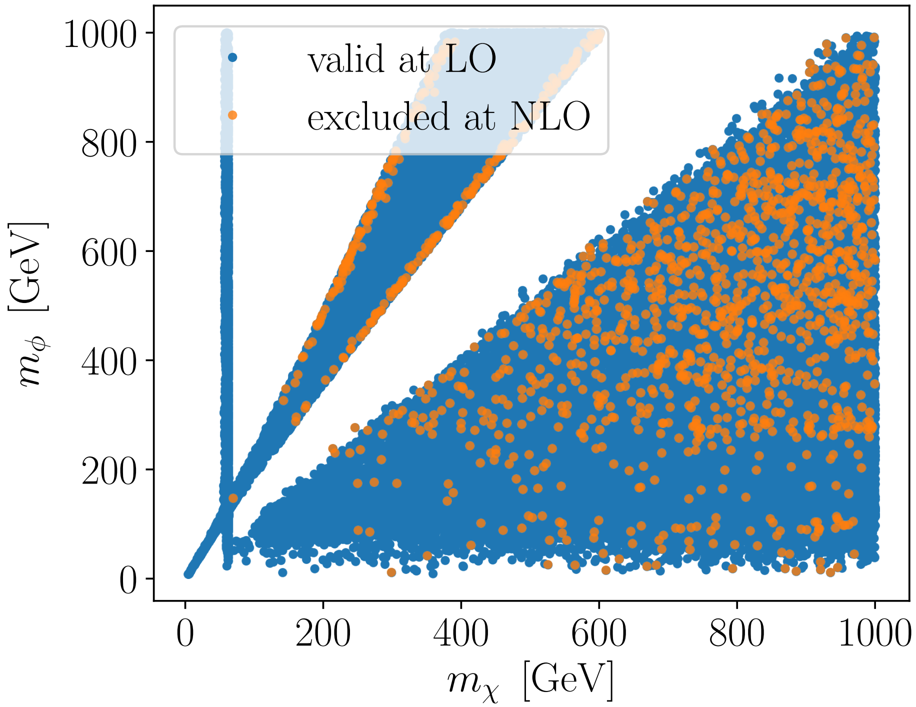

However, when performing a scan there is no noticeable change in the allowed parameter space of the VDM model.

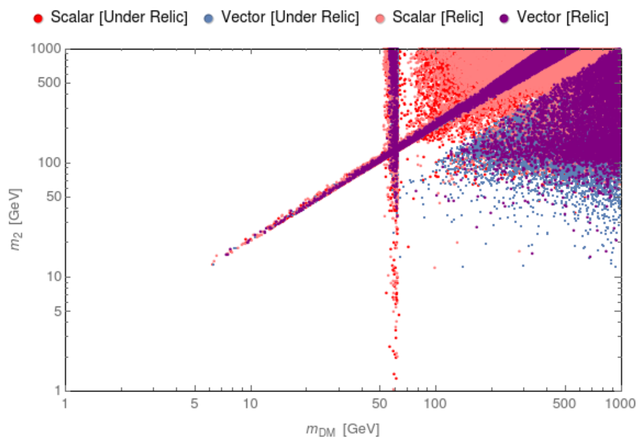

Next: we are generating a sample that has no direct detection constraints to finally see how this changes the different detection regions.

Conclusions

- Can we distinguish a simple SDM from a simple VDM?
- For some pairs of values (m_{DM}, m_2) only the SDM is allowed.

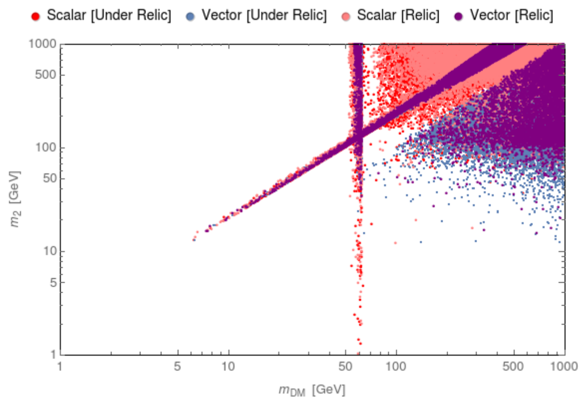

- The reason is the cross section for direct detection - it is several orders of magnitude smaller in the SDM. One-loop corrections (sometimes) matter.

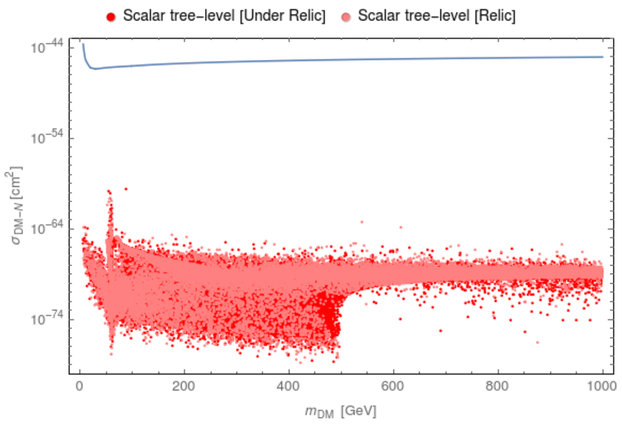

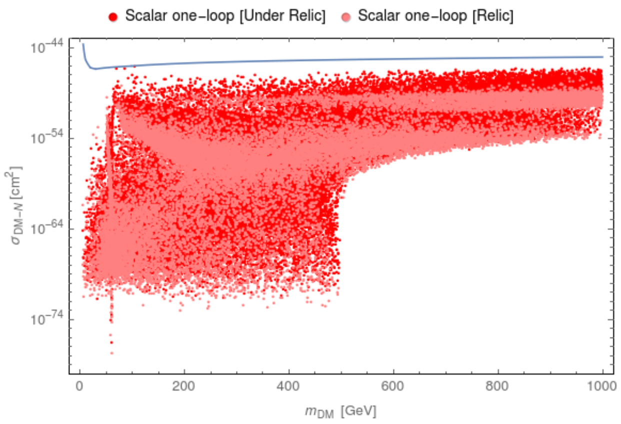

Conclusions

- What about the VDM model? If one chooses a point in parameter space

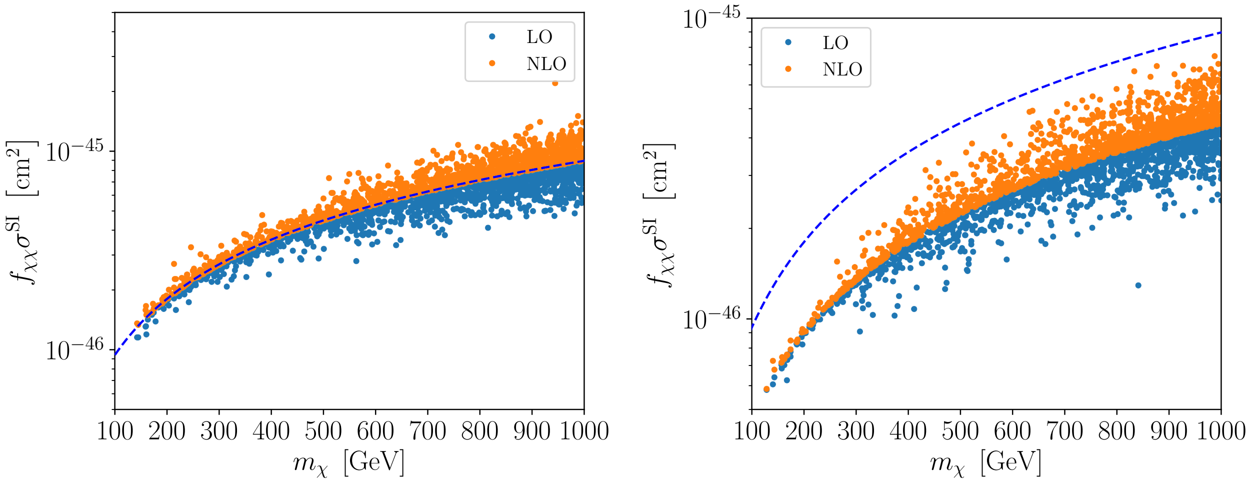

- In a scan

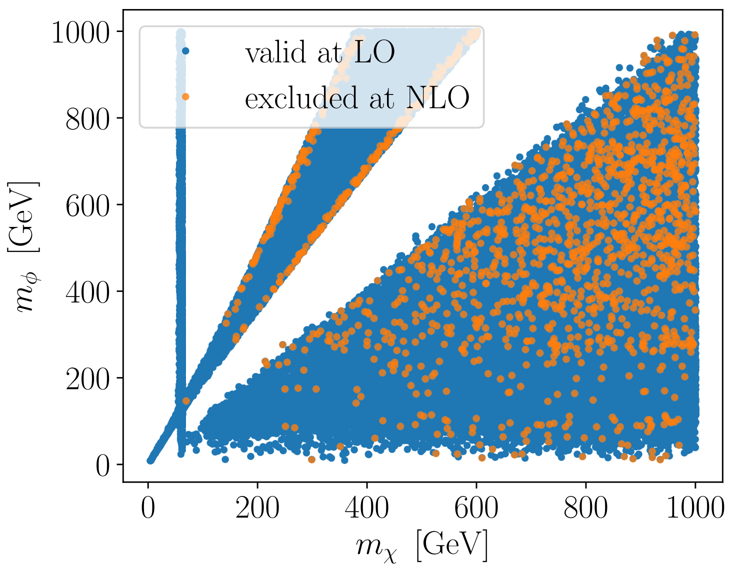

The End

Nuclear form factors

We here present the numerical values for the nuclear form factors defined in Eq. (4.59). The values of the form factors for light quarks are taken from `micrOmegas` [75]

$$f^p_{T_u} = 0.01513\,, \quad f^p_{T_d} = 0.0.0191\,, \quad f^p_{T_s} = 0.0447\,, \tag{A.99a}$$

$$f^n_{T_u} = 0.0110\,, \quad f^n_{T_d} = 0.0273\,, \quad f^n_{T_s} = 0.0447\,, \tag{A.99b}$$

which can be related to the gluon form factors as

$$f^p_{T_G} = 1 - \sum_{q=u,d,s} f^p_{T_q}\,, \qquad f^n_{T_G} = 1 - \sum_{q=u,d,s} f^n_{T_q}\,. \tag{A.100}$$

The needed second momenta in Eq. (4.59) are defined at the scale $\mu = m_Z$ by using the `CTEQ` parton distribution functions [76],

$$u^p(2) = 0.22\,, \qquad \bar{u}^p(2) = 0.034\,, \tag{A.101a}$$

$$d^p(2) = 0.11\,, \qquad \bar{d}^p(2) = 0.036\,, \tag{A.101b}$$

$$s^p(2) = 0.026\,, \qquad \bar{s}^p(2) = 0.026\,, \tag{A.101c}$$

$$c^p(2) = 0.019\,, \qquad \bar{c}^p(2) = 0.019\,, \tag{A.101d}$$

$$b^p(2) = 0.012\,, \qquad \bar{b}^p(2) = 0.012\,, \tag{A.101e}$$

where the respective second momenta for the neutron can be obtained by interchanging up- and down-quark values.